

Evaluation of the Optical Aspects of the Ophthalmic Viscosurgical Device During Femtosecond Laser-Assisted Cataract Surgery

Ho Seok Chung^{1,*}, Jinho Lee^{2,*}, Hun Lee³, Jae Yong Kim³, and Hungwon Tchah^{3,†}

¹ Department of Ophthalmology, Dankook University Hospital, Dankook University College of Medicine, Cheonan, Korea

² The Research Institute of Natural Science and Department of Physics Education, Gyeongsang National University, Jinju, Korea

³ Department of Ophthalmology, College of Medicine, University of Ulsan, Asan Medical Center, Seoul, Korea

Correspondence: Hungwon Tchah, Department of Ophthalmology, Asan Medical Center, University of Ulsan College of Medicine, 88 Olympic-ro 43-gil, Songpa-gu, Seoul 05505, Republic of Korea. e-mail: hwtchah@amc.seoul.kr

Received: October 20, 2021

Accepted: April 7, 2022

Published: May 4, 2022

Citation: Chung HS, Lee J, Lee H, Kim JY, Tchah H. Evaluation of the optical aspects of the ophthalmic viscosurgical device during femtosecond laser-assisted cataract surgery. *Transl Vis Sci Technol.* 2022;11(5):2, <https://doi.org/10.1167/tvst.11.5.2>

Purpose: In femtosecond laser-assisted cataract surgery (FLACS), capsulorhexis can be performed with an ophthalmic viscosurgical device (OVD) filled in the anterior chamber. We aimed to investigate changes in the laser properties in various optical aspects, such as focal shifting, reflection, and absorption associated with OVD.

Methods: Simulation was achieved by calculating the laser power attenuation due to reflection and spot size change using the Gullstrand eye model. Additionally, we calculated the absorption coefficient by measuring the laser power passing through the OVD with a laser meter and evaluated the effect of absorption by the OVD.

Results: In our simulation, power attenuation due to reflection was a maximum of 0.07%, and power attenuation was 0.08% even when considering the change according to the incident angle. Power attenuation due to the change of the spot size at the focus was 0.005%. Owing to the absorption of the OVD, a power increase of up to 13.5% was required for an anterior chamber depth of 3.0 mm to obtain the same effect as the aqueous humor.

Conclusions: The main reason for laser power attenuation associated with OVD was laser absorption through the OVD, and could also be caused by laser cavitation bubbles. To complete a safe capsulotomy during FLACS, the laser power should be increased appropriately, considering the absorption by the OVD in the anterior chamber.

Translational Relevance: The study results can be applied to calculate the optimal femtosecond laser energy to achieve complete capsulotomy during FLACS in the presence of anterior chamber OVD.

Introduction

Femtosecond laser is the latest laser technology using near infrared light, where reflections, absorptions, and focal shifts occur as it passes through a medium, similar to what generally occurs in light. Recently, in the field of ophthalmic surgery, the use of femtosecond laser (center wavelength, $\lambda = 1053 \text{ nm}$) has gradually been gaining popularity worldwide.¹⁻³ The primary advantage of lasers in ophthalmologic surgery is that the laser beam selectively damages the target layer without causing any injury to the other layers, because we can choose an appropriate

wavelength that is transparent for the other layers except the target layer. Furthermore, femtosecond laser-assisted cataract surgery (FLACS) helps continuous curvilinear capsulorhexis to be more rounded and well-centered which, as a result, can be used for safe and accurate cataract surgery.⁴

Cataract surgery in small pupils is associated with an increased incidence of complications, including posterior capsule rupture, due to limited visibility.⁵ When a small pupil is observed prior to cataract surgery, pupil expansion using drugs or ophthalmic viscosurgical devices (OVDs) and mechanical stretching with tools, such as an iris hook, can be considered.⁶ The small pupil is also an issue during FLACS because

capsulorhexis and nuclear fragmentation can damage the pupillary border. Accordingly, a small pupil is considered as a relative contraindication of FLACS⁷ and is significantly challenging in surgery, especially with pupils smaller than 4.6 mm. When a small pupil is observed prior to FLACS, it is difficult to expand the pupil beyond 5.5 mm with intracameral drugs alone; therefore, additional viscomydriasis or mechanical stretching using a pupil expander is required⁸ for most cases of small pupils during FLACS. Viscomydriasis can expand the pupil simply by injecting an OVD into the anterior chamber; if the pupil size exceeds the reference point after viscomydriasis, it is possible to perform capsulorhexis and nuclear fragmentation with the femtosecond laser.^{9,10} In addition, there are case reports introducing FLACS after using a pupil expander in cases of small irregular pupils. Even in these cases, OVD injection is required before the insertion of the pupil expander, and the OVD is maintained in the anterior chamber before the femtosecond laser is applied.¹¹

To avoid surgical complications caused by incomplete capsulorhexis during FLACS after filling the anterior chamber with OVDs, as mentioned in a previous study,⁷ an extensive understanding of laser properties is required. A focal shift difference due to the different refractive indices of OVD has been carefully studied in previous studies, and it was found that this difference in the laser focus had no significant clinical effect.¹²

It is determined that along with the shifting of the laser focus, laser power is also affected by the reflection from the boundaries between the cornea and OVDs, the OVDs and the lens, the spot size at focus, and absorption. This compels for a comprehensive study of all possible optical aspects. Therefore, in this study, the optical effects of the OVD in the anterior chamber on the femtosecond laser was investigated by analyzing the general characteristics of lasers, such as focal shifting, reflection, and absorption. We analyzed the reflection and spot size changes over a range of refractive indices wide enough to cover the various commercial OVDs. To obtain the absorption coefficients, we carefully measured the power attenuations for a few different OVDs and, based on the measurements, were able to evaluate the absorption effect as well.

Methods

Laser Power Measurements Through OVD

We measured laser power and laser pulse energy using a laser energy meter (Coherent; LabMax-TOP, Santa Clara, CA). The total distance from the outlet

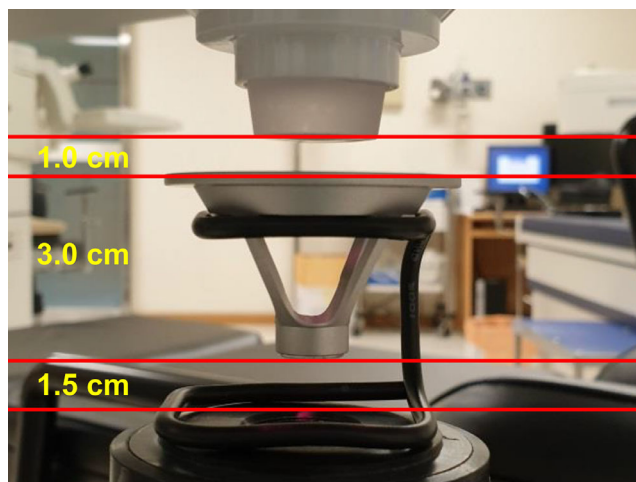


Figure 1. Schematic diagram of measurement of laser power and dimensions for each part.

of the femtosecond laser cataract device (Catalys; Johnson & Johnson, New Brunswick, NJ) to the laser energy meter was 5.5 cm, as shown in [Figure 1](#).

The patient interface appplanation cone used as the precise reference surface in the flap creation of LASIK surgery in the Intralase FS laser was fixed between the laser device and laser energy meter, using a specially made iron bracket. The distances between the laser beam projector and the top of the cone and between the bottom of the cone and the laser energy meter were 1.0 and 1.5 cm, respectively (see [Fig. 1](#)). The cone-shaped structure was observed to be 3 cm high, and a round glass container with a diameter of 11 mm and a thickness of 1.5 mm was placed at the bottom of the cone-shaped structure. We projected 1 μ J of laser energy from the femtosecond laser cataract device and measured the laser power after it passed through water or the OVDs. After filling the cylindrical space above the round glass of the cone with water or OVDs to a height of 1.5 mm or 3.0 mm, the laser power passed was measured. Four different OVDs, including Healon (1.0% sodium hyaluronate; Johnson & Johnson), Healon GV (1.4% sodium hyaluronate; Johnson & Johnson), Healon 5 (2.3% sodium hyaluronate; Johnson & Johnson), and Discovisc (1.6% hyaluronic acid and 4.0% chondroitin sulfate; Alcon, Fort Worth, TX) were used for absorption measurement. The refractive indices for these OVDs are listed in [Table 1](#). We repeated the experiments five times for each material, and the average values were obtained.

Optical Model of the Anterior Segment

To estimate the reflectance, beam size at focus, and absorption, simulations were performed based on the

Table 1. Refractive Index of Water and Ophthalmic Viscosurgical Devices

Materials	Refractive Index ¹³
Healon	1.336 ^a
Healon GV	1.338 ^a
Healon 5	1.338 ^a
Discovisc	1.340 ^a
Cornea	1.376
Aqueous humor	1.336
Lens: Cortex	1.386

^aProvided by the manufacturer.

Gullstrand eye model.¹³ The optical model used in this study ignores high-order aberrations, using the assumption that the contents of the anterior chamber are completely replaced by OVD, and that the size of the cornea and anterior chamber do not change during the procedures.

Simulation of Power Loss from Reflection

To analyze laser power loss at the interface between two different refractive index materials, we used the Fresnel equation at the normal incident, given by the following formula¹⁴:

$$R = \left| \frac{n_t - n_i}{n_t + n_i} \right|^2 \quad (1)$$

where R is the reflectance, and n_i and n_t are the refractive indices of the first and second material, respectively, when the laser travels. In the simulation, three boundaries for reflection (air/anterior cornea, posterior cornea/OVDs, and OVDs/lens) should be considered; however, we did not include the reflection at air/anterior cornea because we filled OVDs in the anterior chamber without affecting the air/anterior cornea boundary. If the reflectance at the first boundary (between posterior cornea and OVD) is R_1 and the remaining $1 - R_1$ travels to the second boundary (between the OVD and the lens), the total reflectance at the two boundaries, R_T , is a simple sum of two reflections, as follows:

$$R_T = R_1 + (1 - R_1) R_2 = R_1 + R_2 - R_1 R_2 \quad (2)$$

where R_2 is the reflectance at the second boundary.

As the reflectance of light depends on the incident angle as well, the spherical shape of the cornea changes the reflectance depending on the radial distance from the spherical center of the cornea. When $R = 6.8 \text{ mm}$, the radius of curvature of the cornea,¹³ and $D = 6 \text{ mm}$, which is a diameter cut by cataract surgery, we get

the maximum 26° incident angle variation by a simple geometric formula, $\theta_i = \sin^{-1} \frac{D}{2R}$. The reflectance with the incident angle can be simulated from the following angle-dependent Fresnel equations¹⁴:

$$R_{\perp} = \left| \frac{\sin(\theta_i - \theta_t)}{\sin(\theta_i + \theta_t)} \right|^2 \quad (3)$$

$$R_{\parallel} = \left| \frac{\tan(\theta_i - \theta_t)}{\tan(\theta_i + \theta_t)} \right|^2 \quad (4)$$

where R_{\perp} , R_{\parallel} are the reflectances perpendicular and parallel to the incident plane, and θ_i and θ_t are the angles of incidence and refraction, respectively. With a given incident angle (θ_i), the refractive angle (θ_t) can be calculated from Snell's law ($n_i \sin \theta_i = n_t \sin \theta_t$, where n_i and n_t are the refractive indices of the incident and refractive domains, respectively). Consequently, Equations 3 and 4 are the functions of one variable, θ_i .

Power Change from Different Spot Size

With a given numerical aperture (NA) of the laser, $NA = \sin \theta = 0.125$ (given by the manufacturer), we calculated half of the converging angle from Snell's law, $\sin \theta_{1/2} = \frac{0.125}{n}$ and obtained a range of 5.21° to 5.37° for refractive indices of OVDs, as listed in Table 1. As the converging angle is related as follows¹⁵:

$$\theta_{1/2} \approx \frac{\lambda}{n\pi\omega_0} \quad (5)$$

we can calculate the beam diameter at the focus using the following relation between the half of the converging angle $\theta_{1/2}$, and the beam waist ω_0 .

$$\omega_0 = \frac{\lambda}{n\pi\theta_{1/2}} = \frac{\lambda}{n\pi \sin^{-1} \frac{0.125}{n}} \quad (6)$$

Power Change from Absorption

Based on the results of the laser power measurement described in the *Laser power measurements through the OVD* section of the Methods, we calculated the absorption coefficient using the following formula¹⁶:

$$I(z) = I_0 e^{-\alpha z} \quad (7)$$

where $I(z)$ is the laser intensity after the traveling distance z ; I_0 and α are the input laser intensity and absorption coefficient of OVD, respectively. The mean anterior chamber depth (ACD) ranged from 3.08 mm to 3.14 mm in other studies,^{17,18} and the ACD in the mid-periphery area where capsulotomy was performed

in FLACS was shallower than in the central area. Using the absorption coefficient of the OVDs calculated from Equation 7, laser power at the anterior capsule of the lens was estimated.

Results

We measured the laser power after passing it through two different lengths (1.5 mm and 3.0 mm) of water and four different OVDs. Additionally, based on Equation 7, we calculated the absorption coefficients for 1.5 mm and 3.0 mm of various materials, as shown in Table 2. The absorption coefficient for the various materials showed the largest values in the following order: Healon 5, Discovisc, Healon, Healon GV, and water.

Figure 2A represents the simulated reflectance based on Equations 1 and 2 at the normal incident for refractive indices of 1.33 to 1.35, covering the aqueous humor and various OVDs. Because the refractive index difference between two materials (posterior cornea/OVDs and OVDs/lens) was relatively small, as mentioned in Table 1, the reflectances for all OVDs, including the aqueous humor, were negligible (in the

order of 10^{-4}). Therefore, the power attenuation from the reflection at the two interfaces was not significant, with a maximum of 0.07%.

To calculate laser power reflection by corneal sphericity, we simulated the change in reflectance according to the radial distance from the central axis of the cornea. For the aqueous humor and Discovisc (the highest refractive index among the OVDs listed in Table 1), we calculated two polarized reflectances R_{\perp} and R_{\parallel} based on Equations 2, 3, and 4. As represented in Figure 2B, only a maximum of 0.08% reflection occurred in both polarizations. Consequently, power attenuation from reflection at different incident angles was not significantly different from the normal incidence, as shown in Figure 2A.

Figure 3A represents a simulated beam diameter at the focus (at the anterior capsule of lens) after passing through various OVDs, using Equation 6.

The equation, $\sin^{-1}x \approx x + \frac{1}{6}x^3 + \dots$, $\omega_0 \approx \frac{\lambda}{n\pi(\frac{1.125}{n} + \frac{1}{6}(\frac{1.125}{n})^3 + \dots)} \approx 0.3\lambda(1 - \frac{0.21}{n^2})$, shows the increase of the beam waist (ω_0), while increasing n . The beam diameter at the focus increased only by 0.01% at the maximum, as shown in Figure 3A. To maintain the same laser effect as the aqueous humor with increased

Table 2. Measured Laser Power and Absorption Coefficient of Water and the Ophthalmic Viscosurgical Devices Depending on the Thickness of Materials

	1.5 mm		3 mm		Average Absorption Coefficient
	Measured Laser Power (μ J)	Absorption Coefficient (mm^{-1})	Measured Laser Power (μ J)	Absorption Coefficient (mm^{-1})	
Water	0.918 ± 0.004	0.0354 ± 0.0064	0.896 ± 0.005	0.0258 ± 0.0032	0.0306
Healon	0.888 ± 0.004	0.0575 ± 0.0064	0.780 ± 0.000	0.0720 ± 0.0034	0.0647
Healon GV	0.898 ± 0.004	0.0500 ± 0.0064	0.808 ± 0.004	0.0620 ± 0.0034	0.0551
Healon 5	0.868 ± 0.004	0.0727 ± 0.0065	0.778 ± 0.004	0.0728 ± 0.0034	0.0728
Discovisc	0.882 ± 0.004	0.0620 ± 0.0065	0.772 ± 0.004	0.0754 ± 0.0034	0.0687

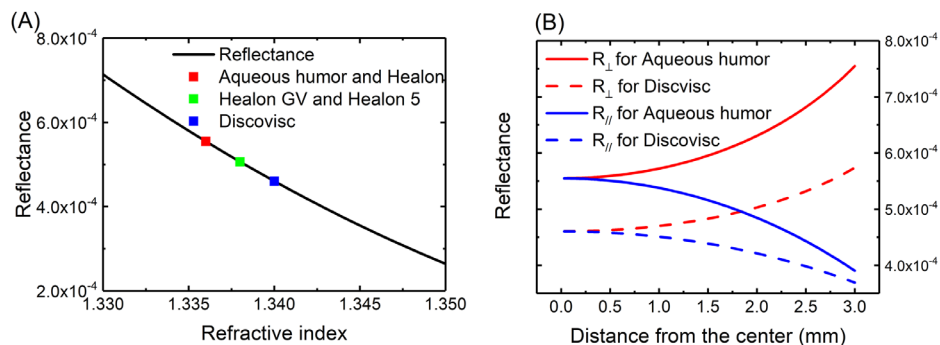


Figure 2. (A) Reflectance at normal incidence according to the refractive indices of various ophthalmic viscosurgical devices. (B) Reflectance of perpendicular (R_{\perp}) and parallel (R_{\parallel}) to the incident plane of laser, according to the various incident angles for aqueous humor and Discovisc.

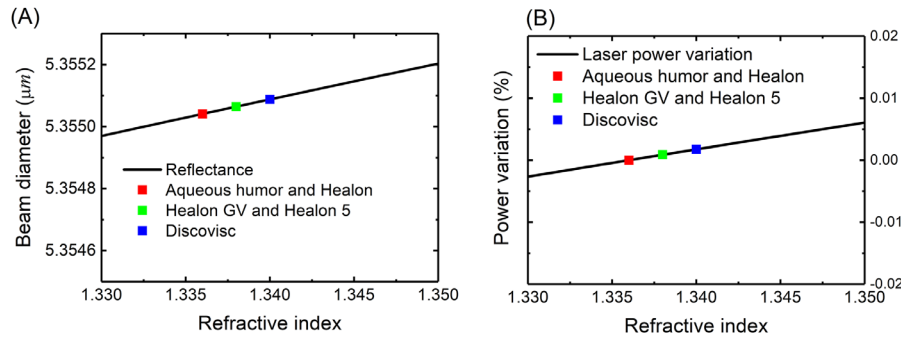


Figure 3. (A) Beam diameter at the focus. (B) Laser power variation according to the refractive indices.

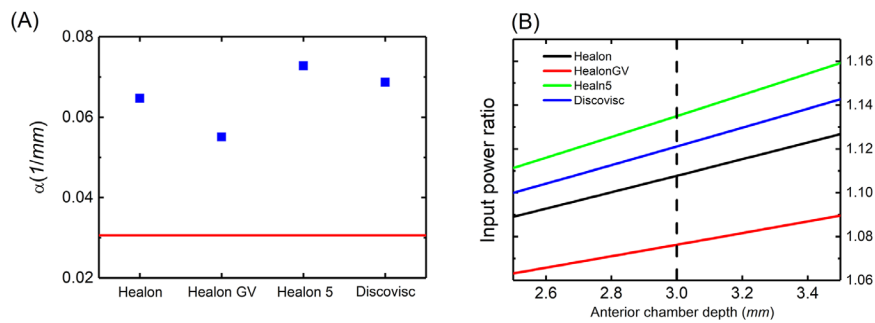


Figure 4. (A) Measured absorption coefficients of various ophthalmic viscosurgical devices and the water (red line). (B) Input laser power ratio to achieve the same power intensity as aqueous humor.

beam diameter, the laser power should be increased up to 0.005%, as shown in Figure 3B, which is negligible.

Figure 4A illustrates the absorption coefficient from our experimental measurements shown in Table 2 to make comparison easier among different materials. Figure 4B shows the input laser power ratio to obtain the same laser effect as when the anterior chamber is filled with the aqueous humor in the ACD of the 2.5 mm to 3.5 mm range, calculated using Equation 7. As shown in Figure 4B, the laser power should be increased by approximately 6% to 16% in different ACDs. For example, in case of an ACD of 3.0 mm, when filling the anterior chamber using Healon, the laser power should be increased by 11% to achieve the same effect as that when the anterior chamber is filled with aqueous humor. Healon 5, which requires the largest power increase in Figure 4B, requires a 13.5% increase in laser power to achieve the same effect at the anterior capsule of the lens.

Discussion

In this study, we measured the laser power after it traveled through OVD to calculate the absorption

coefficient, and simulated changes in the laser power due to reflection, beam size change at focus, and absorption with different OVDs. We found that reflection and beam size change at the focus did not significantly affect laser power. However, due to absorption of the OVD, it was found that a laser power increase of approximately 6% to 16% is required in different ACDs for complete capsulorhexis, depending on the type of OVD.

We analyzed laser power reduction at the boundaries of the posterior cornea/OVDs and OVDs/lens and found a power reduction of 0.07% (see Fig. 2A) at these boundaries. A small difference in the refractive index between the two materials, which is the numerator of the Fresnel equation (see Equation 1), results in a small reflectance. The OVDs in Table 1 had the same refractive index to the first decimal place as the cornea and lens; therefore, we can expect that laser power attenuation due to reflection would be small, as shown in Figure 2A. In addition, the reflection due to the curvature of the cornea was also small, as represented in Figure 2B.

The NA of the laser, $\sin \theta = 0.125$ (converging angle $\approx 14^\circ$) did not significantly change the beam size at the focal point and only a small laser power attenuation (0.005%) was predicted (see Fig. 3A). In a previous

study, it was reported that an overall focal shift of approximately $-8\ \mu\text{m}$ to $13\ \mu\text{m}$ can occur when considering a measurement error of the ACD, and femtosecond laser focal shift due to the refractive index of the OVDs filling the anterior chamber.¹² However, because the default capsulotomy depth of the Catalys was $600\ \mu\text{m}$, and it could be adjusted from $200\ \mu\text{m}$ to $1000\ \mu\text{m}$, we could ignore the focal shift as well. Therefore, we conclude that there are no noticeable effects on laser power attenuation related to the refractive indices of OVDs in Table 1.

We calculated laser power attenuation according to the absorption of the OVDs, using the absorption coefficient obtained from the experimental results. The absorption coefficients were Healon 5, Discovisc, Healon, and Healon GV, in the order of highest absorption, and laser power attenuations were in the same order. Consequently, a power increase of up to 13.5% was required when using the Healon 5 in case of an ACD of 3.0 mm to have the same power as the aqueous humor. A power attenuation of 0.07% due to reflection (ignoring 0.005% due to the beam size change at the focus) and 13.5% power attenuation due to the absorption, results in a total power attenuation of 13.57%. A power attenuation of 13.57% in FLACS is significant and should be considered when the anterior chamber is filled with OVD.

It is worth mentioning that the formation of a cavitation bubble caused by the femtosecond laser should be considered.¹⁹ When an intense laser is focused on any material, a nonlinear optical effect induces optical breakdown and consequently plasma formation. Shock wave emission by plasma expansion generates cavitation bubbles.²⁰ A femtosecond laser would form cavitation bubbles; therefore, power attenuation by cavitation bubbles should be additionally included in actual clinical practice. If the size of the bubble is bigger than the size of the laser spot, power attenuation due to reflection at the two interfaces of the bubble when the laser passes through the cavitation bubble can be approximately estimated. The refractive index inside the cavitation bubble, which is mostly carbon dioxide, is about 1.0, which is significantly different from that of OVD. Based on Equation 1, the reflectance from one interface of the cavitation bubble is approximately 0.02 in case a bubble is surrounded by OVD with a refractive index of 1.336, which corresponds to 2% power attenuation, and 3.9% power is attenuated when passing through one bubble (two interfaces). As a result, power loss increases by the number of bubbles that the laser passes through. Moreover, if the size of the bubble is small enough, light scattering should be considered.

Although it is difficult to quantitatively measure the number, size, and life time of cavitation bubbles, it is reported that the higher the viscosity of OVD, the lower the number and size of bubbles.¹⁹ In a recent study, an incomplete capsulotomy was observed more frequently when using a high-viscosity OVD than when using a low-viscosity OVD, suggesting that high-viscosity OVDs could reduce the efficacy of the femtosecond laser by prolonging the lifetime of the bubble and reducing the impact velocity.^{20,21} Therefore, in addition to our results, the effect of cavitation bubbles should be considered; the relationship between the viscosity of OVD and bubble generation will be investigated through future studies using a streak camera with different laser powers.

In a previous study using porcine eyes, an incomplete capsulotomy occurred less when using 150% of energy compared to when using 90% of energy, and the efficiency of FLACS could be enhanced with high energy in the presence of OVDs.²¹ The authors of the previous study mentioned the possibility of a detrimental effect on capsulotomy formation by cavitation bubbles; however, they did not count the absorption of laser by OVDs. The absorption coefficient is an intrinsic physical property of a material, aside from its refractive index or viscosity, and as 13.5% laser power attenuation is considerably large, absorption through OVDs must be considered. Although the probability of achieving a complete capsulotomy increases when 150% of energy is used, as indicated by results of the previous study,²¹ an increase in laser energy can adversely affect capsulorhexis, such as capsular adhesion and an increased risk of anterior-capsular tags.²² Therefore, it is important to increase laser energy appropriately through accurate calculations. Moreover, considering the results of this study, power attenuation due to absorption must be included in the calculation.

In the application of these findings, it must be considered that ACD differs from person to person and may change during FLACS. In a previous study, the mean ACD was reported to range from 3.08 mm to 3.14 mm using several measurement methods.¹⁷ Another previous study using Scheimpflug imaging found that ACD ranged from 3.09 mm to 3.14 mm in 95% of the participants, albeit there were variances by country.¹⁸ In the present study, a 6% to 16% increase in laser power was required, and the ratio varied with the ACD from 2.5 mm to 3.5 mm. As a result, an exact measurement of the ACD using Scheimpflug or optical coherence tomography before the surgery is required to apply these findings to clinical practice and properly adjust the input laser power.

Because this study was simulated using an optical model, it is assumed that there was no change in

ACD during femtosecond laser surgery. However, in actual surgery, there is a risk of OVD overflow due to negative pressure suction or OVD leaking through the incision made during OVD injection. Although negative pressure suction is required to attach the Catalys femtosecond laser system to the patient's eye, it is attached to the sclera beyond the limbus and the attachment site is made of a silicone tube, which has minimal effect on the OVD in the anterior chamber. In addition, the Catalys femtosecond laser system uses a gentle liquid optic interface to dock to the patient's cornea, which prevents external high pressure or distortion of the cornea.^{23,24} Moreover, a small incision of less than 1 mm was made during the OVD injection into the anterior chamber. As a result, OVD overflow or leakage through the incision might be reduced. Nevertheless, there is a possibility that a small amount of OVD is leaked from the anterior chamber during various processes of real femtosecond laser procedures; therefore, a clinical study to calculate femtosecond laser power in humans will be required to supplement the limitations of the model-based calculations.

In conclusion, we simulated laser power attenuation due to OVD filling the anterior chamber in the possible optical aspects, suggesting that major laser power attenuation could be derived from laser absorption through OVDs and possibly from laser cavitation bubbles, as well. In order to complete a safe capsulotomy during FLACS, it is necessary to increase the laser power appropriately in consideration of the absorption by the OVD filled in the anterior chamber. Although an integrated study of the absorption effect and formation of a cavitation bubble is needed, the absorption of OVDs itself is one of the major factors of power attenuation in FLACS.

Acknowledgments

Supported by Basic Science Research Program through the National Research Foundation of Korea (NRF) funded by the Ministry of Education (grant number: 2021R111A1A01052749).

Conflicting Interests Statement: The authors have no proprietary interest in or financial support for the development or marketing of instruments or equipment mentioned in this article, or for any competing instruments or pieces of equipment.

Disclosure: **H.S. Chung**, None; **J. Lee**, None; **H. Lee**, None; **J.Y. Kim**, None; **H. Tchah**, None

* HSC and JL contributed equally to this work.

References

1. Bali SJ, Hodge C, Lawless M, Roberts TV, Sutton G. Early experience with the femtosecond laser for cataract surgery. *Ophthalmology*. 2012;119(5):891–899.
2. Kolb CM, Shajari M, Mathys L, et al. Comparison of femtosecond laser-assisted cataract surgery and conventional cataract surgery: meta-analysis and systematic review. *J Cataract Refract Surg*. 2020;46:1075–1085.
3. Reddy KP, Kandulla J, Auffarth GU. Effectiveness and safety of femtosecond laser-assisted lens fragmentation and anterior capsulotomy versus the manual technique in cataract surgery. *J Cataract Refract Surg*. 2013;39(9):1297–1306.
4. Zhu Y, Chen X, Chen P, et al. Lens capsule-related complications of femtosecond laser-assisted capsulotomy versus manual capsulorhexis for white cataracts. *J Cataract Refract Surg*. 2019;45(3):337–342.
5. Hashemi H, Seyedian MA, Mohammadpour M. Small pupil and cataract surgery. *Curr Opin Ophthalmol*. 2015;26(1):3–9.
6. Balal S, Jbari AS, Nitiapapand R, et al. Management and outcomes of the small pupil in cataract surgery: iris hooks, Malyugin ring or phenylephrine? *Eye (Lond)*. 2020;35:2714–2718.
7. Donaldson KE, Braga-Mele R, Cabot F, et al. Femtosecond laser-assisted cataract surgery. *J Cataract Refract Surg*. 2013;39(11):1753–1763.
8. Conrad-Hengerer I, Hengerer FH, Schultz T, Dick HB. Femtosecond laser-assisted cataract surgery in eyes with a small pupil. *J Cataract Refract Surg*. 2013;39(9):1314–1320.
9. Goldman JM, Karp CL. Adjunct devices for managing challenging cases in cataract surgery: capsular staining and ophthalmic viscosurgical devices. *Curr Opin Ophthalmol*. 2007;18(1):52–57.
10. Goldman JM, Karp CL. Adjunct devices for managing challenging cases in cataract surgery: pupil expansion and stabilization of the capsular bag. *Curr Opin Ophthalmol*. 2007;18(1):44–51.
11. Roberts TV, Lawless M, Hodge C. Laser-assisted cataract surgery following insertion of a pupil expander for management of complex cataract and small irregular pupil. *J Cataract Refract Surg*. 2013;39(12):1921–1924.
12. de Freitas CP, Cabot F, Manns F, Culbertson W, Yoo SH, Parel JM. Calculation of ophthalmic vis-

- coelastic device-induced focus shift during femtosecond laser-assisted cataract surgery. *Invest Ophthalmol Vis Sci.* 2015;56(2):1222–1227.
13. Jenkins FA, White HE. *Fundamentals of optics.* 4th ed. New York, NY: McGraw-Hill; 1976:190.
 14. Hecht E, Zajac A. *Optics.* 2nd ed. Reading, MA: Addison-Wesley Pub. Co.; 1987:102.
 15. Siegman AE. *Lasers.* Mill Valley, CA: University Science Books; 1986:671–672.
 16. Atkins PW, Atkins PW, De Paula J. *Atkins' Physical chemistry.* 7th ed. New York, NY: Oxford University Press; 2002:479.
 17. Lavanya R, Teo L, Friedman DS, et al. Comparison of anterior chamber depth measurements using the IOLMaster, scanning peripheral anterior chamber depth analyser, and anterior segment optical coherence tomography. *Br J Ophthalmol.* 2007;91(8):1023–1026.
 18. Feng MT, Belin MW, Ambrosio R, Jr., et al. Anterior chamber depth in normal subjects by rotating Scheimpflug imaging. *Saudi J Ophthalmol.* 2011;25(3):255–259.
 19. Dick HB, Schultz T. Laser-assisted cataract surgery in small pupils using mechanical dilation devices. *J Refract Surg.* 2013;29(12):858–862.
 20. Liu X-M, Liu X-H, He J, Hou Y-F, Lu J, Ni X-W. Cavitation bubble dynamics in liquids of different viscosity. *2010 Symposium on Photonics and Optoelectronics: IEEE;* 2010:1–4.
 21. Mansoor H, Liu YC, Wong YR, Lwin NC, Seah XY, Mehta JS. Evaluation of femtosecond laser-assisted anterior capsulotomy in the presence of ophthalmic viscoelastic devices (OVDs). *Sci Rep.* 2020;10(1):21542.
 22. Sandor GL, Kiss Z, Bocskai ZI, et al. Evaluation of the mechanical properties of the anterior lens capsule following femtosecond laser capsulotomy at different pulse energy settings. *J Refract Surg.* 2015;31(3):153–157.
 23. Talamo JH, Gooding P, Angeley D, et al. Optical patient interface in femtosecond laser-assisted cataract surgery: contact corneal applanation versus liquid immersion. *J Cataract Refract Surg.* 2013;39(4):501–510.
 24. Latz C, Asshauer T, Rathjen C, Mirshahi A. Femtosecond-Laser Assisted Surgery of the Eye: Overview and Impact of the Low-Energy Concept. *Micromachines (Basel).* 2021;12(2):122.